IEEE Control Systems Letters paper presented at
2023 62nd IEEE Conference on Decision and Control (CDC)
December 13-15, 2023. Marina Bay Sands, Singapore

Robust Constraint-Following Control for Uncertain Mechanical Systems with Generalized Udwadia-Kalaba Approach

Zicheng Zhu, Jun Ma, Wenxin Wang, Yuanjie Xian, Hao Sun, Han Zhao, and Tong Heng Lee

***Abstract*— In this letter, we propose a robust constraint-following control approach for uncertain mechanical systems under both equality and inequality constraints. Particularly, both the global and local inequality constraints are systematically incorporated into the Udwadia-Kalaba (U-K) equation leveraging the diffeomorphism technique, wherein a novel smooth approximation of the local inequality constraints is proposed to address the non-differentiability resulting from its spatiotemporal dependence nature. Based on this development, the generalized U-K equation is mathematically established. With this, we develop a robust constraint-following control strategy to ensure satisfying system performance in the presence of uncertainties and various constraints. Moreover, by Lyapunov minimax approach, the proposed control strategy guarantees both uniform boundedness (UB) and uniform ultimate boundedness (UUB) of the system. Finally, numerical simulations on the lateral motion control of an autonomous vehicle demonstrate the effectiveness of the proposed approach.**

I. INTRODUCTION

Robust stability and performance of servo mechanical systems have gathered significant research attention in the existing literature [1]. The primary motivation for its development is to analyze and design a control strategy to mitigate the influence of system uncertainty. Since the uncertainty in mechanical system dynamics is generally time-varying, designers typically use its bound as the basis for controller design to ensure satisfactory system performance. Along with this line, substantial efforts have been devoted to the development of robust control strategies [2]–[4]. Specifically for servo mechanical systems, most existing works on robust control mainly focus on trajectory tracking and set-point stabilization problems. In realistic scenarios, specific nonholonomic constraints are commonly encountered in these control problems, which are not investigated thoroughly.

Constraint-following control, inspired by the servo constraint problem in analytical mechanics, has been one of the research frontiers in control systems [5]–[7]. Specifically, the implementation of constraint-following control via the Udwadia-Kalaba (U-K) approach facilitates the management of both holonomic and nonholonomic constraints in servo mechanical systems [8]. In addition, this method does not require any linearizations or nonlinear cancellations for the mechanical systems. It also renders the control input to meet Gauss's principle and D'Alembert's principle, thus generating a moderate control force in the real world. Furthermore, the U-K approach does not require any auxiliary variables (such as Lagrange multiplier) or pseudo variables (such as generalized speeds) compared with the standard Lagrange equation. Apart from equality constraints, a series of inequality constraints also need to be satisfied due to physical limitations, prescribed performance, and safety specifications of servo mechanical systems. Since an added control force introduced by inequality constraints can impede the equality constraint-following performance and increase the complexity of control problems, it brings additional challenges to the control design.

To ensure the satisfaction of inequality constraints and maintain the stability, barrier Lyapunov functions (BLFs) have been widely applied in control systems [9]–[11]. In [11], an adaptive neural network control methodology was developed by utilizing BLF to deal with the system constraints and disturbances. Another effective tool to handle the inequality constraints in mechanical systems is the diffeomorphism approach, which transforms the state from bounded space to an unbounded counterpart [12]. In [13], a diffeomorphism-based robust bounded control scheme was formulated to address the inequality constraints in the trajectory tracking task. Furthermore, in certain instances, the inequality constraints are spatiotemporally dependent, i.e., only activated when the controlled system enters a specific area or time interval, which are the so-called local inequality constraints. Local inequality constraints are inherently nondifferentiable due to their piecewise nature resulting from spatiotemporal dependence, which renders the control problem rather difficult to be solved. However, in most of the existing efforts, only global constraints (i.e., the constraints exist throughout the entire domain) are considered in the trajectory tracking problems. In this sense, it leaves an open and interesting question to handle local inequality constraints

This work was supported in part by the China Scholarship Council under Grant 202206690023; and in part by the Project of Hetao Shenzhen-Hong Kong Science and Technology Innovation Cooperation Zone under Grant HZQB-KCZYB-2020083. *(Corresponding author: Jun Ma.)*

Zicheng Zhu and Yuanjie Xian are with the School of Mechanical Engineering, Hefei University of Technology, Hefei 230009, China, and also with the Department of Electrical and Computer Engineering, National University of Singapore, Singapore 117583. {zhuzicheng, xianyuanjie}@u.nus.edu.

Jun Ma is with the Robotics and Autonomous Systems Thrust, The Hong Kong University of Science and Technology (Guangzhou), Guangzhou, China, also with the Division of Emerging Interdisciplinary Areas, The Hong Kong University of Science and Technology, Hong Kong SAR, China, and also with the HKUST Shenzhen-Hong Kong Collaborative Innovation Research Institute, Futian, Shenzhen, China. jun.ma@ust.hk.

Wenxin Wang and Tong Heng Lee are with the Department of Electrical and Computer Engineering, National University of Singapore, Singapore 117583. wenxin.wang@u.nus.edu, eleleeth@nus.edu.sg.

Hao Sun and Han Zhao are with the School of Mechanical Engineering, Hefei University of Technology, Hefei, Anhui 230009, China. {sunhao.0806, hanzhao}@hfut.edu.cn.

as typically encountered in servo mechanical systems.

This work proposes a novel perspective on the U-K approach for handling both equality and inequality constraints in uncertain mechanical systems, which is distinctly different from existing approaches in [10], [14]–[16]. Leveraging the diffeomorphism technique and a smooth approximation, both the global and local inequality constraints are systematically incorporated into the constraint-following problem. Then, effective extensions are made to the existing U-K approach and the generalized U-K equation is established therein. By Lyapunov minimax approach, the proposed robust controller guarantees both uniform boundedness (UB) and uniform ultimate boundedness (UUB) of the servo mechanical system even in the presence of uncertainties. Particularly, different from [14], [15], the diffeomorphism of this work is constraint-based and does not invoke the complicated state transformation to the system equation. In contrast with [10], the applicability of the proposed robust controller is not only limited to autonomous systems, but also can be utilized for non-autonomous systems, such that time-varying uncertainty can be dealt with appropriately. Although the barrier function used in [16] is effective in addressing inequality constraints, this method primarily does not provide effective routines for handling various types of equality constraints, especially non-holonomic equality constraints. However, our approach inherits the advantages of the U-K approach, especially the ability to deal with both holonomic and nonholonomic equality constraints. In summary, this work establishes a systematic framework for handling (i) both holonomic and nonholonomic constraints; (ii) both equality and inequality constraints; (iii) both global and local inequality constraints; (iv) both autonomous and non-autonomous systems.

II. Problem Formulation

A. System Description

The dynamical model of an uncertain mechanical system can be given by the following equation:

$$\begin{aligned} &M(\nu(t),\varpi(t),t)\ddot{\nu}(t)+C(\nu(t),\dot{\nu}(t),\varpi(t),t)\dot{\nu}(t)\\ &+G(\nu(t),\varpi(t),t)+F(\nu(t),\dot{\nu}(t),\varpi(t),t)=u(t), \end{aligned} \tag{1}$$

where $t\in\mathbf{R}$ is the time, $\nu\in\mathbf{R}^n$, $\dot{\nu}\in\mathbf{R}^n$, and $\ddot{\nu}\in\mathbf{R}^n$ represent the position, the velocity, and the acceleration, respectively. The vector $\varpi(t)\in\Pi\subset\mathbf{R}^q$ denotes the possibly fast time-varying uncertainty with the compact bounding set Π. Also, M represents the inertia matrix, C represents the Coriolis or centrifugal force, G represents the force of gravity, and F is the impressed forces except for the force of gravity. The vector $u\in\mathbf{R}^n$ is the control input.

Consider that the system (1) is subject to the following constraint in the first-order form [15]:

$$D(\nu,t)\dot{\nu}=c(\nu,t), \tag{2}$$

where $D=[D_{pi}]_{m\times n}$ and $c=[c_1\ c_2\dots c_m]^T$. The constraint (2) may be holonomic and/or nonholonomic. Then, by taking time-derivative of (2), the second-order form of the constraints is given as

$$D(\nu,t)\ddot{\nu}=b(\nu,\dot{\nu},t), \tag{3}$$

where $b=[b_1\ b_2\dots b_m]^T$.

Assumption 1 [5]: (i) For each $(\nu,t)\in\mathbf{R}^n\times\mathbf{R}$, $\mathrm{rank}[D(\nu,t)]\geq 1$ and $D(\nu,t)$ is of full rank; (ii) For each $(\nu,t)\in\mathbf{R}^n\times\mathbf{R}$, $\varpi\in\Pi$, $M(\nu,\varpi,t)>0$.

Let $F_{eq}=C\dot{\nu}+G+F$, we have the following theorem:

Theorem 1 [15]: Consider the system (1) and the servo constraint (3) are subject to Assumption 1, with the U-K equation, the constraint force is given as

$$\begin{aligned} Q^c=&M^{\frac{1}{2}}(\nu,\varpi,t)(D(\nu,t)M^{-\frac{1}{2}}(\nu,\varpi,t))^{\dagger}[b(\nu,\dot{\nu},t)\\ &+D(\nu,t)M^{-1}(\nu,\varpi,t)F_{eq}(\nu,\dot{\nu},\varpi,t)], \end{aligned} \tag{4}$$

where the superscript "†" represents the Moore-Penrose (MP) generalized inverse.

Remark 1: This work relies on the U-K approach which is well-suited for addressing the inherent nonlinearity of the mechanical systems, and it provides an explicit closed-form constraint force. This may not be straightforward to obtain using linearization-based methods. In the absence of consideration for uncertainty, utilizing $u=Q^c$ would be sufficient to accurately drive the system to follow the specified servo constraint (3). Nevertheless, as parameter uncertainties and external disturbances inevitably exist, it is critical to design a robust control scheme that guarantees constraint-following performance under various uncertainties.

B. Diffeomorphism for Inequality Constraints

In practice, the system is typically under the following global inequality constraints:

$$\underline{\phi}_j(\nu,t)<\phi_j(\nu,t)<\bar{\phi}_j(\nu,t),\ j=1,2,\dots,l, \tag{5}$$

where $\underline{\phi}_j(\nu,t)$ and $\bar{\phi}_j(\nu,t)$ are C^1 in ν and t, representing the upper and lower bounds for $\phi_j(\nu,t)$.

By using the U-K equation, it is only possible to follow the servo equality constraint (3) through the design of the constraint force (4). Hence, to satisfy the specified inequality constraints, an additional constraint force Q^i is formulated:

$$Q^i(\nu,\dot{\nu},t)=(I-D^{\dagger}(\nu,t)D(\nu,t))r(\nu,\dot{\nu},t), \tag{6}$$

where $r(\nu,\dot{\nu},t)\in\mathbf{R}^n$ is a vector that is used to adjust the magnitude of the additional constraint force Q^i. Recalling the property of MP inverse, by (1) and (4), we have

$$\begin{aligned} D\ddot{\nu}=&D[M^{-\frac{1}{2}}(DM^{-\frac{1}{2}})^{\dagger}(b+DM^{-1}F_{eq})-M^{-1}F_{eq}+Q^i]\\ =&b+(D-DD^{\dagger}D)r=b. \end{aligned} \tag{7}$$

This implies that the constraint (3) is still guaranteed under the addition of Q^i.

Following it, we aim to design a local diffeomorphism to transform the constrained space of $\phi_j(\nu,t)$ to an unconstrained counterpart. Thus, solving the inequality constraint problem is converted to find a sequence of Ξ_j such that for $\phi_j(\nu,t)\in\Omega_j=(\underline{\phi}_j,\bar{\phi}_j)$, the local diffeomorphism satisfies

$\Xi_j : \Omega_j \to \mathbf{R},\ j = 1, 2, \ldots, l$. Based on the above analysis, we propose the following diffeomorphism:

$$\xi_j = \text{artanh}\left[\frac{2}{\bar{\phi}_j - \underline{\phi}_j}\phi_j(\nu,t) + \frac{\bar{\phi}_j + \underline{\phi}_j}{\bar{\phi}_j - \underline{\phi}_j}\right] + \lambda_j =: s_j(\nu,t), \tag{8}$$

where ξ_j is the transformed variable and the parameter λ_j is used to adjust the correspondence between ξ_j and ϕ_j in the diffeomorphism. Notice that $\xi_j \to +\infty$ when $\phi_j(\nu,t) \to \bar{\phi}_j$ and $\xi_j \to -\infty$ when $\phi_j(\nu,t) \to \underline{\phi}_j$.

Additionally, the system is possibly subject to a class of local inequality constraints. That is, $\phi_j(\nu,t) \in (\underline{\phi}_j, \bar{\phi}_j)$ for $\varepsilon_j \in (\underline{\varepsilon}_j, \bar{\varepsilon}_j)$, $j = 1, 2, \ldots, p$. Notice that ε_j here is a general symbol. It could refer to the state variable ν_j or time variable t. To address the non-differentiability of the local equality constraint, a smooth approximation is appropriately constructed as follows:

$$\bar{\phi}^j_{ap}(\nu,t) := \frac{1}{\beta_1}e^{\beta_2(\varepsilon_j - \underline{\varepsilon}_j)(\varepsilon_j - \bar{\varepsilon}_j)} - \frac{1}{\beta_1} + \bar{\phi}_j(\nu,t), \tag{9}$$

$$\underline{\phi}^j_{ap}(\nu,t) := -\frac{1}{\beta_1}e^{\beta_2(\varepsilon_j - \underline{\varepsilon}_j)(\varepsilon - \bar{\varepsilon}_j)} + \frac{1}{\beta_1} + \underline{\phi}_j(\nu,t). \tag{10}$$

Note that the functions (9) and (10) are smooth and differentiable. Here, $\beta_1, \beta_2 > 0$ are the smoothing parameters and the approximation effect improves as they increase.

Consider both global and local inequality constraints, with the diffeomorphism (8), the relation between the original coordinate ν and the transformed coordinate ξ is given as

$$\xi = s(\nu,t), \tag{11}$$

where $\xi = [\xi_1\ \xi_2 \cdots \xi_l]^T$ and $s = [s_1\ s_2 \cdots s_l]^T$. Then, we proceed to take the first-order and second-order time derivatives of (11), which yields

$$\dot{\xi} = \frac{\partial s}{\partial \nu}\dot{\nu} + \frac{\partial s}{\partial t},\ \ddot{\xi} =: h_1(\nu,\dot{\nu},t) + h_2(\nu,\dot{\nu},t)r, \tag{12}$$

where

$$h_1(\nu,\dot{\nu},t) = \left[\frac{d}{dt}\left(\frac{\partial s}{\partial \nu}\right)\right]\dot{\nu} + \frac{\partial^2 s}{\partial t^2} + \left(\frac{\partial s}{\partial \nu}\right)[-M^{-1}F_{eq} + M^{-\frac{1}{2}}(DM^{-\frac{1}{2}})^\dagger(b + DM^{-1}F_{eq})], \tag{13}$$

$$h_2(\nu,\dot{\nu},t) = \left(\frac{\partial s}{\partial \nu}\right)(I - D^\dagger D). \tag{14}$$

Referring to (12), we define $\tilde{\zeta} := \xi$ and $\hat{\zeta} := \dot{\xi}$. Let $\zeta := [\tilde{\zeta}^T\ \hat{\zeta}^T]^T$, $h_3(\nu,\dot{\nu},t) := [\hat{\zeta}^T\ h_1^T(\nu,\dot{\nu},t)]^T$, and $h_4(\nu,\dot{\nu},t) := [\mathbf{0}_{n\times l}\ h_2^T(\nu,\dot{\nu},t)]^T$. The second-order derivative of ξ can be equivalently represented as $\dot{\zeta} = h_3(\nu,\dot{\nu},t) + h_4(\nu,\dot{\nu},t)r$.

Assumption 2: There exist a vector $r_0(\nu,\dot{\nu},t) : \mathbf{R}^n \times \mathbf{R}^n \times \mathbf{R} \to \mathbf{R}^n$, a continuously differentiable function $V(\cdot) : \mathbf{R}^{2l} \times \mathbf{R} \to \mathbf{R}_+$, and scalar constants $\gamma_{1,2} \geq 0$, $\tilde{h} \geq 0$ such that for all $\|\zeta\| > \tilde{h}$, $\gamma_1\|\zeta\|^2 \leq V(\zeta,t) \leq \gamma_2\|\zeta\|^2$ and $\frac{\partial V(\zeta,t)}{\partial t} + \nabla_\zeta^T V(\zeta,t)(h_3(\nu,\dot{\nu},t) + h_4(\nu,\dot{\nu},t)r_0(\nu,\dot{\nu},t)) \leq 0$.

The implication of this assumption is that ζ is bounded by choosing an appropriate vector r_0. With $\zeta = [\xi^T\ \dot{\xi}^T]^T$, this in turn means ξ is bounded. Therefore, by designing the diffeomorphism (8), which indicates that $\xi_j \to +\infty$ as $\phi_j(\nu,t) \to \bar{\phi}_j$ and $\xi_j \to -\infty$ as $\phi_j(\nu,t) \to \underline{\phi}_j$, the prescribed inequality constraint can be strictly satisfied.

When the system uncertainty is known a priori, recalling the constraint force (4) and the design of Q^i, the generalized U-K equation considering both equality servo constraints and inequality constraints is formulated as

$$M\ddot{\nu} = -F_{eq} + M^{\frac{1}{2}}(DM^{-\frac{1}{2}})^\dagger(b + DM^{-1}F_{eq}) + M(I - D^\dagger D)r_0. \tag{15}$$

III. Robust Control Design

For the uncertain system (1), we have the following decomposition: $M(\nu,\varpi,t) = \bar{M}(\nu,t) + \Delta M(\nu,\varpi,t)$, $C(\nu,\dot{\nu},\varpi,t) = \bar{C}(\nu,\dot{\nu},t) + \Delta C(\nu,\dot{\nu},\varpi,t)$, $G(\nu,\varpi,t) = \bar{G}(\nu,t) + \Delta G(\nu,\varpi,t)$, $F(\nu,\dot{\nu},\varpi,t) = \bar{F}(\nu,\dot{\nu},t) + \Delta F(\nu,\dot{\nu},\varpi,t)$. With $\bar{M} > 0$, let $E := \bar{M}^{-1}$, $\Delta E := M^{-1} - \bar{M}^{-1}$, and $\Lambda := \bar{M}M^{-1} - I$. Thus, we have $\Delta E := E\Lambda$.

Assumption 3: There exists a constant $\rho_\Lambda > -1$ such that for all $(\nu,t) \in \mathbf{R}^n \times \mathbf{R}$,

$$\frac{1}{2}\min_{\varpi\in\Pi}\lambda_m(\Lambda(\nu,\varpi,t) + \Lambda^T(\nu,\varpi,t)) \geq \rho_\Lambda. \tag{16}$$

It should be noted that the control objective of a servo mechanical system is to follow the prescribed constraints (2). With this, we define $\eta(\nu,\dot{\nu},t) := D(\nu,t)\dot{\nu} - c(\nu,t)$, which serves as one of the metrics of the constraint-following performance.

With the decomposition of matrices, we define $\bar{F}_{eq} := \bar{C}\dot{\nu} + \bar{G} + \bar{F}$ and $\Delta F_{eq} := \Delta\bar{C}\dot{\nu} + \Delta\bar{G} + \Delta\bar{F}$. Then, the η-dynamics is given as

$$\dot{\eta} = D(Eu - E\bar{F}_{eq} - E\Delta F_{eq} + \Delta E(u - F_{eq})) - b. \tag{17}$$

Assumption 4: There exist a constant $\gamma \in \mathbf{R}_+$ and a function $g(\gamma,\cdot) : \mathbf{R}_+ \times \mathbf{R}^m \times \mathbf{R} \to \mathbf{R}^m$ such that the function $g(\gamma,\cdot) \in \mathfrak{R}(D)$. Also, there exist a Lyapunov function $\mathcal{L}(\cdot) : \mathbf{R}^m \times \mathbf{R} \to \mathbf{R}_+$, and constants $c_i > 0$, $i = 1, 2, 3$ such that for all $(\gamma,\nu,\dot{\nu},t) \in \mathbf{R}_+ \times \mathbf{R}^n \times \mathbf{R}^n \times \mathbf{R}$,

$$c_1\|\eta\|^2 \leq \mathcal{L}(\eta,t) \leq c_2\|\eta\|^2, \tag{18}$$

$$\frac{\partial\mathcal{L}(\eta,t)}{\partial t} + \nabla_\eta^T\mathcal{L}(\eta,t)g(\gamma,\eta,t) \leq -\gamma c_3\|\eta\|^2. \tag{19}$$

where $\mathfrak{R}(\cdot)$ denotes the range space of a matrix. Inspired by the generalized U-K equation (15), we propose

$$u_1 := \bar{M}^{\frac{1}{2}}(D\bar{M}^{-\frac{1}{2}})^\dagger(g + b + D\bar{M}^{-1}\bar{F}_{eq}) + \bar{M}(I - D^\dagger D)r_0. \tag{20}$$

Theorem 2: Consider the nominal part of the system (1), for all $(\gamma,\nu,\dot{\nu},\eta,t) \in \mathbf{R}_+ \times \mathbf{R}^n \times \mathbf{R}^n \times \mathbf{R}^m \times \mathbf{R}$, given the function $g(\gamma,\eta,t) = -\epsilon\gamma\eta$ with a constant $\epsilon > 0$, the control $u = u_1(\gamma,\nu,\dot{\nu},\eta,t)$ renders the origin of the nominal η-dynamics globally asymptotically stable and $\lim_{t\to\infty}\eta = 0$.

Proof: By (17), the nominal η-dynamics can be written as

$$\dot{\eta} = D(Eu - E\bar{F}_{eq}) - b. \tag{21}$$

With $u = u_1$ and the property of MP inverse, we have

$$D(Eu - E\bar{F}_{eq}) - b$$

$$=D\bar{M}^{-\frac{1}{2}}(D\bar{M}^{-\frac{1}{2}})^{\dagger}(g+b+D\bar{M}^{-1}\bar{F}_{eq}))-D\bar{M}^{-1}\bar{F}_{eq}-b$$
$$=g+b+D\bar{M}^{-1}\bar{F}_{eq}-D\bar{M}^{-1}\bar{F}_{eq}-b=g. \quad (22)$$

Choose the Lyapunov function $\mathcal{L}_1=\eta^T\eta/2$, and the derivative of $\mathcal{L}_1$ yields

$$\dot{\mathcal{L}}_1=\eta^T\dot{\eta}=\eta^T[D(Eu-E\bar{F}_{eq})-b]$$
$$=\eta^T g=-\epsilon\gamma\|\eta\|^2\leq 0. \quad (23)$$

Therefore, the control u_1 guarantees that the origin $\eta=0$ of nominal η-dynamics is a globally asymptotically stable equilibrium point and η converges to zero as $t\to\infty$. ■

Remark 3: Theorem 2 indicates that the control u_1 only compensates the nominal dynamics of η. Hence, to additionally compensate for the uncertain part of the η-dynamics, another term u_2 needs to be introduced in the control u.

Assumption 5 [13]: There exist an unknown scalar α and a known function $\Sigma(\cdot)\in\mathbf{R}_+$ such that for all $(\gamma,\nu,\dot{\nu},\eta,t)\in\mathbf{R}_+\times\mathbf{R}^n\times\mathbf{R}^n\times\mathbf{R}^m\times\mathbf{R}$, $\varpi\in\Pi$,

$$\|\Lambda(\nu,\varpi,t)(-F_{eq}(\nu,\dot{\nu},\varpi,t)+u_1(\gamma,\nu,\dot{\nu},\eta,t))$$
$$-\Delta F_{eq}(\nu,\dot{\nu},\varpi,t)\|\leq\alpha\Sigma(\gamma,\nu,\dot{\nu},\eta,t). \quad (24)$$

Next, the robust control scheme is proposed as follows:

$$u=u_1(\gamma,\nu,\dot{\nu},\eta,t)+u_2(\gamma,\nu,\dot{\nu},\eta,t), \quad (25)$$

with $u_2(\gamma,\nu,\dot{\nu},\eta,t)=-\kappa\mu\|\mu\|^{2\rho-2}\Sigma^{2\rho}(\gamma,\nu,\dot{\nu},\eta,t)$ and $\mu=ED^T\nabla_\eta\mathcal{L}$. Also, $\kappa>0$ and $\rho>1$ are scalar constants.

Theorem 3: Consider that the system (1) is subject to Assumptions 1-5. The control law (25) renders η uniformly bounded and uniformly ultimately bounded.

Proof: We proceed to prove Theorem 3 based on the Lyapunov minimax approach. By (17) and (25), the first-order derivative of $\mathcal{L}$ can be given as

$$\dot{\mathcal{L}}=\frac{\partial\mathcal{L}}{\partial t}+\nabla_\eta^T\mathcal{L}\dot{\eta}=\frac{\partial\mathcal{L}}{\partial t}+\nabla_\eta^T\mathcal{L}[D(-E\bar{F}_{eq}+E(u_1+u_2)$$
$$-E\Delta F_{eq}+\Delta E(-F_{eq}+u_1+u_2))-b]. \quad (26)$$

By (19) and (22), we have

$$\frac{\partial\mathcal{L}}{\partial t}+\nabla_\eta^T\mathcal{L}[D(-E\bar{F}_{eq}+Eu_1)-b]\leq-\gamma c_3\|\eta\|^2. \quad (27)$$

Since $\Delta E:=E\Lambda$, with $\mu=ED^T\nabla_\eta\mathcal{L}$ and (24), we have

$$\nabla_\eta^T\mathcal{L}D(\Delta E(-F_{eq}+u_1)-E\Delta F_{eq})\leq\alpha\|\mu\|\Sigma. \quad (28)$$

Recall the design of u_2, and we have

$$\nabla_\eta^T\mathcal{L}D(E+\Delta E)u_2$$
$$=-\kappa\|\mu\|^{2\rho}\Sigma^{2\rho}+\nabla_\eta^T\mathcal{L}DE\Lambda(-\kappa\mu\|\mu\|^{2\rho-2}\Sigma^{2\rho}). \quad (29)$$

By (16), the second term of (29) yields

$$\nabla_\eta^T\mathcal{L}DE\Lambda(-\kappa\mu\|\mu\|^{2\rho-2}\Sigma^{2\rho})$$
$$=-\frac{1}{2}\kappa\nabla_\eta^T\mathcal{L}DE(\Lambda+\Lambda^T)ED^T\nabla_\eta\mathcal{L}\|\mu\|^{2\rho-2}\Sigma^{2\rho}$$
$$\leq-\kappa\rho_\Lambda\|\mu\|^{2\rho}\Sigma^{2\rho}. \quad (30)$$

Substituting (30) into (29), we have

$$\nabla_\eta^T\mathcal{L}D(E+\Delta E)u_2\leq-\kappa(1+\rho_\Lambda)\|\mu\|^{2\rho}\Sigma^{2\rho}. \quad (31)$$

Combining (27), (28), and (31), thus we have

$$\dot{\mathcal{L}}\leq-\gamma c_3\|\eta\|^2+\alpha\|\mu\|\Sigma-\kappa(1+\rho_\Lambda)\|\mu\|^{2\rho}\Sigma^{2\rho}$$
$$=:-\gamma c_3\|\eta\|^2+\lambda_1, \quad (32)$$

where $\lambda_1=(2\rho-1)\alpha^{\frac{2\rho}{2\rho-1}}\sqrt[2\rho-1]{\alpha/(2\rho\kappa(1+\rho_\Lambda))}/2\rho$. It concludes that $\dot{V}<0$ for all $\|\eta\|>\sqrt{\lambda_1/\gamma c_3}$. Therefore, the control law (25) ensures UB and UUB of the vector η. ■

IV. Illustrative Example

A. System Description

The lateral motion control of an autonomous vehicle is used as an illustrative example in this section. In this example, the vehicle aims to traverse the local area while maintaining a constant longitudinal velocity, and not exceeding the roadside line. Then, the equation of motion in the lateral and yaw directions can be written as

$$\begin{bmatrix}m&0\\0&J\end{bmatrix}\begin{bmatrix}\ddot{y}\\\ddot{\psi}\end{bmatrix}+\begin{bmatrix}\frac{C_f+C_r}{v}&\frac{C_fl_f-C_rl_r}{v}+mv\\\frac{C_fl_f-C_rl_r}{v}&\frac{C_fl_f^2+C_rl_r^2}{v}\end{bmatrix}\begin{bmatrix}\dot{y}\\\dot{\psi}\end{bmatrix}$$
$$=\begin{bmatrix}F_{xf}+C_f&F_{xr}+C_r\\(F_{xf}+C_f)l_f&-(F_{xr}+C_r)l_r\end{bmatrix}\begin{bmatrix}\delta_f\\\delta_r\end{bmatrix}, \quad (33)$$

where y is the lateral position of the vehicle, ψ is the yaw angle, m denotes the vehicle mass, J denotes the moment of inertia, C_f, C_r denote the cornering stiffness of the front tire and the rear tire, l_f, l_r denote the distances from center of gravity to the front axle and the rear axle, F_{xf}, F_{xr} denote the longitudinal forces of the front tires and the rear tires, respectively, δ_f, δ_r denote the front and rear steering angles, v is the longitudinal velocity of the vehicle.

To ensure that the safety and comfort of passengers in on-road driving scenarios, the reference commands regarding the yaw angle and yaw rate are given as $\psi_r=0$ and $\dot{\psi}_r=0$. Furthermore, to ensure the tracking error is approximately asymptotically stable, we formulate the trajectory constraint as $(\dot{\psi}-\dot{\psi}_r)+\lambda(\psi-\psi_r)=0$, where $\lambda>0$ is a scalar constant. Then, the constraint can be rewritten into the second-order form (3), which yields $D=[0\ 1]$ and $b=\ddot{\psi}_r-\lambda(\dot{\psi}-\dot{\psi}_r)$.

Furthermore, to avoid possible collisions in the locally bounded area, we suppose that the vehicle is under the following inequality constraint:

$$\underline{y}+\frac{w}{2}<y<\bar{y}-\frac{w}{2},\ \text{for}\ \underline{x}<x<\bar{x}, \quad (34)$$

where w is the width of the vehicle. Also, $\bar{x}$, $\underline{x}$, $\bar{y}$, and $\underline{y}$ are constants which specify the scope of the local region. For the numerical simulation, we choose $w=1.786$ m, $\bar{y}=1$ m, $\underline{y}=-1$ m, $\bar{x}=20$ m, and $\underline{x}=10$ m. Since a constant longitudinal velocity is assumed, $x\in(\underline{x},\bar{x})$ indeed corresponds to $t\in(\underline{x}/v,\bar{x}/v)$. Following (9) and (10), the approximation can be formulated as $\underline{y}_{ap}=-\frac{1}{\beta_1}e^{\beta_2(t-\underline{x}/v)(t-\bar{x}/v)}+\frac{1}{\beta_1}+\underline{y}+\frac{w}{2}$ and $\bar{y}_{ap}=\frac{1}{\beta_1}e^{\beta_2(t-\underline{x}/v)(t-\bar{x}/v)}-\frac{1}{\beta_1}+\bar{y}-\frac{w}{2}$ with $\beta_1=1\times10^4$ and $\beta_2=5$.

Recalling (8), the following diffeomorphism is formulated to address the inequality constraint (34), which yields

$$\xi=\text{artanh}\left(\frac{2}{\bar{y}_{ap}-\underline{y}_{ap}}y\right)=:\text{artanh}(\kappa_1 y). \quad (35)$$

B. Assumption Verification

(i) Verification on Assumptions 1-3: Note that $\text{rank}[D] = 1$, and it is straightforward that D is of full rank. It follows that Assumption 1 is satisfied with the vehicle mass $m > 0$ and the moment of inertia $J > 0$. Recall that $D = [0\ 1]$, with $r_0 = [r_1\ r_2]^T$, we have $(I - D^\dagger D)r_0 = [r_1\ 0]^T$. With (12) and $h_2 = [\tilde{h}_2\ 0]$, then we have

$$\dot{\xi} = \frac{\dot{\kappa}_1 y + \kappa_1 \dot{y}}{1 - (\kappa_1 y)^2},\ \ddot{\xi} = h_1 + \tilde{h}_2 r_1, \tag{36}$$

where

$$h_1 = \frac{(\ddot{\kappa}_1 y + 2\dot{\kappa}_1 \dot{y})(1 - \kappa_1^2 y^2) + 2\kappa_1 y(\dot{\kappa}_1 y + \kappa_1 \dot{y})^2}{(\kappa_1^2 y^2 - 1)^2} + \frac{\kappa_1(C_f + C_r)\dot{y} + \kappa_1(C_f l_f - C_r l_r)\dot{\psi} + \kappa_1 \bar{m} v^2 \dot{\psi}}{\bar{m} v(\kappa_1 y)^2 - \bar{m} v}, \tag{37}$$

$$\tilde{h}_2 = \frac{\kappa_1}{1 - (\kappa_1 y)^2}. \tag{38}$$

Since $-1 < \kappa_1 y < 1$, then $1 - (\kappa_1 y)^2 > 0$. With $r_0 = [r_1^*\ 0]^T$, we choose $r_1^* = -\frac{h_1 + k_1\xi + k_2\dot{\xi}}{\tilde{h}_2}$, where k_1 and k_2 are positive constants. Substituting $r_1 = r_1^*$ into (36), thus we have $\ddot{\xi} = -k_1\xi - k_2\dot{\xi}$. It is straightforward to verify Assumption 2 and ξ is thus bounded.

We recall that $E := \bar{M}^{-1}$, $\Delta E := M^{-1} - \bar{M}^{-1}$, and $\Lambda := \bar{M}M^{-1} - I$. For the autonomous vehicle, we have $\Lambda = \Lambda^T = \text{diag}[\bar{m}/m - 1,\ \bar{J}/J - 1]$. Then, we have $\frac{1}{2}\min\lambda_m(\Lambda + \Lambda^T) = \min\{\bar{m}/m - 1,\ \bar{J}/J - 1\}$. Since $m > 0$, $\bar{m} > 0$, $J > 0$, and $\bar{J} > 0$, it follows that $m/\bar{m} > 0$ and $J/\bar{J} > 0$. Therefore, $m/\bar{m} - 1 > -1$ and $J/\bar{J} - 1 > -1$, which implies that $\frac{1}{2}\min\lambda_m(\Lambda + \Lambda^T) > -1$. Hence, there always exists a constant $\rho_\Lambda > -1$ that meets Assumption 3. Here, we choose $\rho_\Lambda = -0.1$.

(ii) Verification on Assumptions 4-5: The function $\mathcal{L}$ represents the Lyapunov function. We choose a standard quadratic Lyapunov function $\mathcal{L} = \eta^T P \eta$ in this design with $P \in \mathbf{R}^{m\times m}$, $P > 0$. Then, Assumption 4 can be met with $c_1 = \lambda_m(P)$, $c_2 = \lambda_M(P)$, and $c_3 = \epsilon\lambda_M(P)$.

We define $\Phi := \|\Lambda(-F_{eq} + u_1) - \Delta F_{eq}\|$. Recalling Assumption 5, the scalar α and Σ are related to the bound of Φ. Thus, we have

$$\Phi \le |\Delta m/m| \underbrace{\left| \bar{m} r_1 - (C_f + C_r)\dot{y}/v - (C_f l_f - C_r l_r)\dot{\psi}/v \right|}_{d_1} + 2\,|\Delta m| \underbrace{\left| v\dot{\psi} \right|}_{d_2} + |\Delta J| \underbrace{|g + b|}_{d_3}. \tag{39}$$

Thus, Assumption 5 can be satisfied with

$$\alpha := \sqrt{\Delta m^2/m^2 + 4\Delta m^2 + \Delta J^2}, \tag{40}$$

$$\Sigma := \sqrt{d_1^2 + d_2^2 + d_3^2}. \tag{41}$$

For the control parameters, we choose $\kappa = \gamma = 2$, $\rho = 2$, $\lambda = 4$, $k_1 = 20$, $k_2 = 5$, $P = 0.005$, and $\epsilon = 1$. For the numerical simulation, the system's parameters are given as $\bar{m} = 800$ kg, $\bar{J} = 1100$ kg $\cdot$ m^2, $C_f = C_r = 20000$ N/rad, $F_{xf} = F_{xr} = 80000$ N, $v = 10$ m/s, $l_f = 1.2247$ m, and $l_r = 1.4373$ m. Also, the system uncertainties are simulated by using parametric variations $\Delta m = |100\sin(10\pi t)|$ kg and $J = 200\sin(20\pi t)$ kg $\cdot$ m^2, and input disturbances $\Delta\delta_f = |\pi/20\sin(4\pi t)|$ rad and $\Delta\delta_r = \pi/20\sin(4\pi t)$ rad.

C. Simulation Results

To verify that the proposed method can satisfy the inequality constraint with the design of diffeomorphism (35), the proposed method without diffeomorphism is used for comparison. Moreover, to evaluate the robustness of our method, we carried out a comparison with the standard linear quadratic regulator (LQR) under identical parametric variations and input disturbances. The initial value for y, $\dot{y}$, ψ, and $\dot{\psi}$ are set as $y(0) = 1$ m, $\dot{y}(0) = -6$ m/s, $\psi(0) = \pi/6$ rad, and $\dot{\psi}(0) = -1.6$ rad/s. For the implementation of LQR, we chose the weighting matrices Q and R as $Q = \text{diag}[3,\ 2,\ 0.01,\ 1]$ and $R = 5$. These values were chosen to ensure that the vehicle tracks the desired reference with the control input remaining within a feasible range of $\delta_f, \delta_r \in (-\pi/4\text{ rad}, \pi/4\text{ rad})$.

Fig. 1 depicts the trajectory of the vehicle. The prescribed local inequality constraint (34) is highlighted in Fig. 1 with a light green rectangular region. It can be seen that when $10 \le x \le 20$, the designed smooth approximation closely fits the actual constraint. In addition, when $x < 10$ or $x > 20$, the approximation rapidly grows exponentially to infinity. This closely adheres to the specified inequality constraint, without affecting the vehicle motion in other regions. From Figs. 1 and 2(a)-(b), the proposed method can effectively address the initial condition deviation of y, while also fulfilling the prescribed constraint. It should be noted that the proposed controller without diffeomorphism and LQR cannot directly handle the constraint. Hence, instead of the inequality constraint, we additionally set the reference command as $y = 0$ and $\dot{y} = 0$ to provide a fair comparison. We can see from Figs. 2(a)-(b) that both the proposed method without diffeomorphism and LQR can converge y and $\dot{y}$ to a small neighborhood near 0. Nevertheless, the actual trajectory exceeds the upper bound line (e.g., between $x = 10$ m and $x = 12$ m), which leads to a collision of the vehicle. As shown in Figs. 2(c)-(d), the proposed methodology drives the vehicle to follow the reference command (i.e., $\psi = 0$ and $\dot{\psi} = 0$), even in the presence of parametric variations and input disturbances. It shows that the proposed robust scheme renders a smaller UUB ball size than that under the proposed controller without diffeomorphism, which indicates a superior tracking performance. However, LQR exhibits more chattering when confronted with various uncertainties due to its insufficient robustness. The actual control inputs are presented in Fig. 3, respectively.

To summarize and compare the preceding simulation results, the accumulative tracking error (ATE) and the accumulative control effort (ACE) of each method are shown in TABLE I. It is evident that the proposed robust control scheme has the lowest ATE and smallest ACE compared with other methods. In summary, leveraging the diffeomorphism technique and constraint-following methodology, the

proposed robust control scheme guarantees the prescribed inequality constraints, attains superior tracking performance, and demonstrates strong robustness despite the presence of various uncertainties.

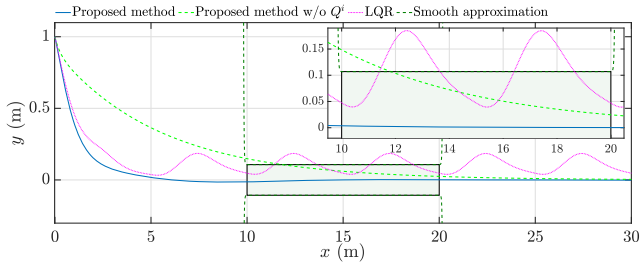

Fig. 1. Comparison of trajectory of the vehicle.

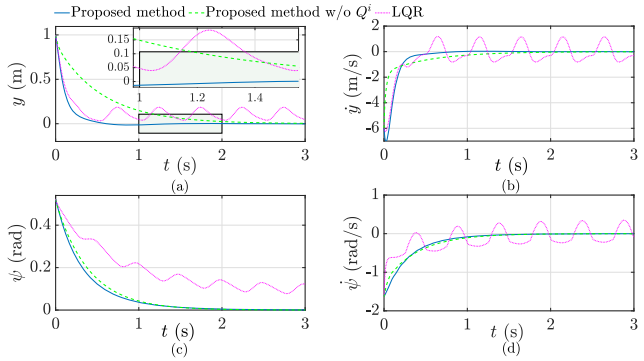

Fig. 2. (a) Comparison of time history of y; (b) Comparison of time history of $\dot{y}$; (c) Comparison of time history of ψ; (d) Comparison of time history of $\dot{\psi}$.

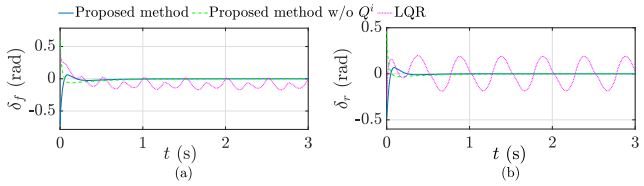

Fig. 3. (a) Comparison of time history of δ_f; (b) Comparison of time history of δ_r.

TABLE I
PERFORMANCE COMPARISON

	ATE (e_ψ)	ATE ($e_{\dot{\psi}}$)	ACE (δ_f)	ACE (δ_r)
Proposed method	0.1874	0.5230	0.0308	0.0209
Proposed method w/o diffeomorphism	0.2060	0.5247	0.0427	0.0245
LQR	0.5668	0.7596	0.2872	0.3396

V. CONCLUSIONS

To address the constraints and uncertainties in servo mechanical systems, this letter developed a robust constraint-following control strategy. Leveraging the diffeomorphism approach, the inequality constraints are systematically incorporated into the U-K equation. With the use of the MP generalized inverse, the generalized U-K equation is effectively established to cope with both the global and local inequality constraints. Based on this, a robust constraint-following control scheme was designed to ensure UB and UUB. Additionally, the stability is strictly guaranteed by the proposed robust control strategy. In summary, this work expands the scope of the U-K equation and provides a new perspective on the management of inequality constraints and uncertainties of servo mechanical systems. Also, it should be noted that the proposed constraint-following controller involves multiple control parameters that significantly influence the constraint-following performance and control cost. This introduces a potential multi-objective and multi-parameter optimization problem among these conflicting criteria. Thus, one possible future work along this line is to investigate a game-theoretic framework to address the control parameter optimization and further enhance the system performance.

REFERENCES

[1] G. Flores, A. M. de Oca, and A. Flores, "Robust nonlinear control for the fully actuated hexa-rotor: Theory and experiments," *IEEE Control Systems Letters*, vol. 7, pp. 277–282, 2023.

[2] E. Vladu and A. Rantzer, "H-infinity control with nearly symmetric state matrix," *IEEE Control Systems Letters*, vol. 6, pp. 3026–3031, 2022.

[3] D. Larby and F. Forni, "A passivity preserving H-infinity synthesis technique for robot control," in *2022 IEEE 61st Conference on Decision and Control (CDC)*, 2022, pp. 1416–1422.

[4] Z. Feng, M. Yu, S. A. Evangelou, I. M. Jaimoukha, and D. Dini, "Mu-synthesis PID control of full-car with parallel active link suspension under variable payload," *IEEE Transactions on Vehicular Technology*, vol. 72, no. 1, pp. 176–189, 2023.

[5] R. Zhao, Y.-H. Chen, and S. Jiao, "Optimal design of constraint-following control for fuzzy mechanical systems," *IEEE Transactions on Fuzzy Systems*, vol. 24, no. 5, pp. 1108–1120, 2016.

[6] Q. Sun, G. Yang, X. Wang, and Y.-H. Chen, "Designing robust control for mechanical systems: Constraint following and multivariable optimization," *IEEE Transactions on Industrial Informatics*, vol. 16, no. 8, pp. 5267–5275, 2020.

[7] Z. Yang, J. Huang, H. Yin, D. Yang, and Z. Zhong, "Path tracking control for underactuated vehicles with matched-mismatched uncertainties: An uncertainty decomposition based constraint-following approach," *IEEE Transactions on Intelligent Transportation Systems*, vol. 23, no. 8, pp. 12 894–12 907, 2022.

[8] Z. Hu, J. Huang, Z. Yang, and Z. Zhong, "Embedding robust constraint-following control in cooperative on-ramp merging," *IEEE Transactions on Vehicular Technology*, vol. 70, no. 1, pp. 133–145, 2021.

[9] Y. Zhang, X. Wang, and Z. Wang, "Adaptive state safety control design for uncertain discrete-time nonlinear systems," *IEEE Control Systems Letters*, vol. 6, pp. 2246–2251, 2022.

[10] L. Liu, Y.-J. Liu, A. Chen, S. Tong, and C. P. Chen, "Integral barrier lyapunov function-based adaptive control for switched nonlinear systems," *Science China Information Sciences*, vol. 63, pp. 1–14, 2020.

[11] R. Rout, R. Cui, and Z. Han, "Modified line-of-sight guidance law with adaptive neural network control of underactuated marine vehicles with state and input constraints," *IEEE Transactions on Control Systems Technology*, vol. 28, no. 5, pp. 1902–1914, 2020.

[12] W. Qin, W.-B. Shangguan, H. Yin, Y.-H. Chen, and J. Huang, "Constraint-following control design for active suspension systems," *Mechanical Systems and Signal Processing*, vol. 154, p. 107578, 2021.

[13] Z. Zhu, H. Zhao, H. Sun, and K. Shao, "Diffeomorphism-based robust bounded control for permanent magnet linear synchronous motor with bounded input and position constraints," *IEEE Transactions on Industrial Informatics*, vol. 19, no. 4, pp. 5387–5399, 2023.

[14] D. Feliu-Talegon, J. Á. Acosta, and A. Ollero, "Control aware of limitations of manipulators with claw for aerial robots imitating bird's skeleton," *IEEE Robotics and Automation Letters*, vol. 6, no. 4, pp. 6426–6433, 2021.

[15] H. Sun, L. Tu, L. Yang, Z. Zhu, S. Zhen, and Y.-H. Chen, "Adaptive robust control for nonlinear mechanical systems with inequality constraints and uncertainties," *IEEE Transactions on Systems, Man, and Cybernetics: Systems*, vol. 53, no. 3, pp. 1761–1772, 2023.

[16] K. Shao, J. Zheng, H. Wang, X. Wang, R. Lu, and Z. Man, "Tracking control of a linear motor positioner based on barrier function adaptive sliding mode," *IEEE Transactions on Industrial Informatics*, vol. 17, no. 11, pp. 7479–7488, 2021.